Prepared for submission to JHEP

# Extraction of $|V_{cb}|$ from $B \to D^{(*)}\ell\nu_\ell$ and the Standard Model predictions of $R(D^{(*)})$

**Sneha Jaiswal,Soumitra Nandi and Sunando Kumar Patra**

*Indian Institute of Technology, North Guwahati, Guwahati 781039, Assam, India*

*E-mail:* sneha.jaiswal@iitg.ernet.in, soumitra.nandi@iitg.ernet.in, sunando.patra@gmail.com

Abstract: We extract $|V_{cb}|$ from the available data in the decay $B \to D^{(*)}\ell\nu_\ell$. Our analysis uses the $q^2(w)$ binned differential decay rates in different subsamples of $B \to D\ell\nu_\ell$ ($\ell = e, \mu$), while for the decay $B \to D^*\ell\nu_\ell$, the unfolded binned differential decay rates of four kinematic variables including the $q^2$ bins have been used. In the CLN and BGL parameterizations of the form factors, the combined fit to all the available data along with their correlations yields $|V_{cb}| = (39.77 \pm 0.89) \times 10^{-3}$ and $(40.90 \pm 0.94) \times 10^{-3}$ respectively. In these fits, we have used the inputs from lattice and light cone sum rule (LCSR) along with the data. Using our fit results and the HQET relations (with the known corrections included) amongst the form factors, and parameterizing the unknown higher order corrections (in the ratios of HQET form factors) with a conservative estimate of the normalizing parameters, we obtain $R(D^*) = 0.259 \pm 0.006$ (CLN) and $R(D^*) = 0.257 \pm 0.005$ (BGL).

arXiv:1707.09977v2 [hep-ph] 26 Nov 2017

## Contents


**1 Introduction** **1**

**2 Inputs** **3**

**3 CLN parameterization : Fit results** **4**
- 3.1 Fit from $B \to D\ell\nu_\ell$ data 4
- 3.2 Fit from $B \to D^*\ell\nu_\ell$ data 5
- 3.3 Combined fit from $B \to D\ell\nu_\ell$ and $B \to D^*\ell\nu_\ell$ data: 7
  - 3.3.1 $R(D^*)$ with the additional error $\Delta$ 9

**4 BGL parametrization** **10**
- 4.1 Formalism and Results for $|V_{cb}|$ 10
- 4.2 Predictions for $R(D^{(*)})$ 12

**5 Summary** **20**

**6 Acknowledgement** **21**


## 1 Introduction

One of the primary goals of the study of $B$ meson decays and mixing is to construct the unitarity triangle (UT). In this regard, the CKM elements $V_{ub}$ and $V_{cb}$ play an important role. Hence, precise measurements of these elements are of utmost importance.

The tree level semileptonic decays $b \to c\ell\nu_\ell$ ($\ell = e, \mu$) are crucial for the determination of $|V_{cb}|$. It can be extracted from both exclusive decays, like $B \to D^{(*)}\ell\nu$, and inclusive decays, like $B \to X_c\ell\nu_\ell$. The inclusive channels are relatively clean, and the decay rates have a solid description via operator product expansion (OPE) or heavy quark expansion (HQE) [1]. The exclusive semileptonic decays have similar solid descriptions in terms of heavy quark effective theory (HQET) [2]. Contrary to the inclusive decays, the non-perturbative unknowns in the exclusive decays can not be extracted experimentally. One needs to calculate them and that is where the major challenges lie. At the moment, the most precise determinations of $|V_{cb}|$ from inclusive [3] and exclusive decays [4] differ from each other at $\approx 3\sigma$ confidence level (CL). Recently it has been shown that the Caprini-Lellouch-Neubert (CLN) [5] and Boyd-Grinstein-Lebed (BGL) [6] parameterizations lead to different results for the exclusive determinations of $|V_{cb}|$ [7]. In their analysis they have used up-to-date lattice calculations of the form factors along with the available experimental results from Belle [8].

Form factors, fitted from the decays $B \to D^{(*)}\ell\nu$, play a crucial role in the Standard Model (SM) predictions of $R(D^{(*)}) = Br(B \to D^{(*)}\tau\nu_\tau)/Br(B \to D^{(*)}\ell\nu)$. In the decays

$B \to D^{(*)}\tau\nu_\tau$, there are additional form factors that can not be extracted directly from the available data on $B \to D^{(*)}\ell\nu$. Therefore, one needs to rely on various theory inputs, the HQET relations between the form factors in particular. The SM predictions of $R(D^{(*)})$ using the CLN parametrization of the form factors and the inputs from lattice and HQET are given by [9, 10]

$$R(D) = 0.300 \pm 0.008, \qquad R(D^*) = 0.252 \pm 0.003. \tag{1.1}$$

Recently, the SM prediction of $R(D)$ has been updated [11] using the lattice input on the form factors in $B \to D\ell\nu_\ell$ beyond the zero recoil [12, 13]. The updated value is $R(D) = 0.299 \pm 0.003$ [11], which is the most precise estimate so far. Also, $R(D^*)$ and $|V_{cb}|$ have been updated from a combined fit to the $B \to D^{(*)}\ell\nu$ differential rates and angular distributions, including $\mathcal{O}(\Lambda_{QCD}/m_{b,c}, \alpha_s)$ terms in HQET form factors [14]. They have obtained

$$|V_{cb}| = (39.3 \pm 1.0) \times 10^{-3}, \qquad R(D^*) = 0.257 \pm 0.003 \tag{1.2}$$

using the lattice results on the form factors and the QCD sum rule (QCDSR) predictions [15, 16] for the HQET parameter as inputs in their analysis. The ratio of the form factors $R_0(w)$ [5, 10], where $w$ is the recoil angle between $B$ and $D^*$, and its value at zero recoil, $R_0(1)$, play a crucial role in the determination of $R(D^*)$. The estimate of $R_0(1)$ depends on the HQET parameter $\eta(1)$, for which the QCDSR prediction is available [14]. However, it is also possible to fit it directly from the available experimental data and the lattice inputs. As an example, we can see the Table-II of ref. [14], and note that the fit results for $\eta(1)$ (with lattice as input) deviates from that predicted in QCDSR by more than $1\sigma$. Also, the ratio of the form factors in $B \to D^{(*)}\ell\nu_\ell$ differ from that predicted by lattice [11, 17]. Therefore, the legitimate query is whether this is due to the missing pieces in the HQET relations between the form factors (i.e. corrections at order $\alpha_s^2$ and $\Lambda_{QCD}^2/m_{b,c}^2$).

In this article, we have extracted $|V_{cb}|$ independently from the fits to the available data on the differential rates and angular distributions in $B \to D\ell\nu_\ell$ and $B \to D^*\ell\nu_\ell$, using the CLN and BGL parameterization of the form factors. We have then performed a combined analysis of the complete data set in both the parameterizations of the form factors and extracted $|V_{cb}|$, $R(D)$ and $R(D^*)$. In this analysis, along with the experimental data, we use the lattice predictions for the form factors as inputs [12, 13].

As mentioned earlier, we have an additional form factor in $R(D^*)$, that cannot be constrained from experimental data alone and we need additional theory inputs. In order to predict $R(D^*)$, we define the HQET relations between the form factors with the known corrections [5, 14], which are represented in terms of the sub-leading Isgur-Wise functions. We constrain those functions (HQET parameters) from a fit to the ratios of the form factors used in our analysis, and the synthetic data for these ratios are obtained using directly our fit results or from lattice and light cone sum rule (LCSR). We repeat the analysis by considering additional parameters ($\Delta$) parameterizing the missing higher order corrections in the ratios of the HQET form factors, and have made a rough estimate of the probable size of these $\Delta$s in different ways with the available resources. We have considered the additional errors conservatively while predicting the SM value of $R(D^*)$.

| $f_+(w)$ & $f_0(w)$ | Value from HPQCD | Correlation | | | | | |
|---|---|---|---|---|---|---|---|
| $f_+(1)$ | 1.178(46) | 1. | 0.994 | 0.975 | 0.507 | 0.515 | 0.522 |
| $f_+(1.06)$ | 1.105(42) | | 1. | 0.993 | 0.563 | 0.576 | 0.587 |
| $f_+(1.12)$ | 1.037(39) | | | 1. | 0.617 | 0.634 | 0.649 |
| $f_0(1)$ | 0.902(41) | | | | 1. | 0.997 | 0.988 |
| $f_0(1.06)$ | 0.870(39) | | | | | 1. | 0.997 |
| $f_0(1.12)$ | 0.840(37) | | | | | | 1. |
| | Value from MILC | | | | | | |
| $f_+(1)$ | 1.1994(95) | 1. | 0.967 | 0.881 | 0.829 | 0.853 | 0.803 |
| $f_+(1.08)$ | 1.0941(104) | | 1. | 0.952 | 0.824 | 0.899 | 0.886 |
| $f_+(1.16)$ | 1.0047(123) | | | 1. | 0.789 | 0.890 | 0.953 |
| $f_0(1)$ | 0.9026(72) | | | | 1. | 0.965 | 0.868 |
| $f_0(1.08)$ | 0.8609(77) | | | | | 1. | 0.952 |
| $f_0(1.16)$ | 0.8254(94) | | | | | | 1. |

**Table 1**: Lattice QCD results of $f_+$ and $f_0$ for different values of $w$. The upper half of the table have been obtained using the fit results from the HPQCD collaboration [13], and the lower half are the results obtained by the Fermilab MILC collaboration [12].

## 2 Inputs

For $B \to D\ell\nu_\ell$ data, we depend on the latest fully reconstructed measurement from Belle [18], but instead of the combined result of 10 $w$ bins (in table II of that paper), we use the full dataset including all the four subsamples $B^+ \to \bar{D}^0 e^+\nu_e$, $B^+ \to \bar{D}^0\mu^+\nu_\mu$, $B^0 \to D^- e^+\nu_e$, and $B^0 \to D^-\mu^+\nu_\mu$, with 40 data-points, along with their statistical and systematic uncertainties and the full systematic correlation matrix. These are available in [20]. We also use the values of the form factors $f_+$ and $f_0$ at $w$ values 1, 1.08, and 1.16 with the full covariance matrix supplied by MILC [12]. On the other hand, the HPQCD collaboration uses BCL parametrization to present their results. While using the HPQCD results [13], we recognize (following the observation made by ref. [11]) that their simulations extend to a maximal value of $z = 0.013$ ($w \approx 1.11$), and thus use synthetic data for $f_{+,0}$ at $w = 1.00,\ 1.06$, and 1.12. These are listed in table 1, with their uncertainties and correlation matrix. Belle, however, has used the same $w$ points as MILC to calculate HPQCD synthetic data in their analysis. We will explicitly mention our inputs whenever we are using them.

| Source | $\mathcal{G}(1)$ |
|---|---|
| Fermilab/MILC [12] | 1.0541(83) |
| HPQCD [13] | 1.035(40) |
| HQE(BPS Expansion) [21] | 1.04(2) |

**Table 2**: Different values of $\mathcal{G}(1)$ used in $B \to D\ell\nu_\ell$ fits.

In addition to using the dispersions relations, CLN parametrization [5] uses Heavy Quark Effective Theory (HQET) to strengthen the unitarity bounds and as a consequence

this establishes approximate relations between the slope and the higher power coefficients of the form factors (valid within $\approx 2\%$). Other than $|V_{cb}|$, only two parameters parametrize the form factors under this scenario: $\rho_D^2$ and $\mathcal{G}(1)$. The form factor normalization $\mathcal{G}(1)$ is predicted by both HPQCD and Fermilab/MILC. There is one HQE result based on Bogomol'nyi-Prasad-Sommerfield (BPS) symmetry (partially)[21] as well. These are listed in table 2 and $\mathcal{G}(1)$ is used as a nuisance parameter in some of our fits.

In our analysis, for the $B \to D^* \ell \nu_\ell$ data, we mainly depend on the unfolded binned differential decay rates by Belle. For four kinematic variables $w$, $\cos\theta_v$, $\cos\theta_l$ and $\chi$, with 10 bins each, this amounts to a total of 40 data points, their uncertainties and the full correlation matrix [8]. Other than these, we make use of the zero-recoil value of the form factor $h_{A_1}(w)$ from unquenched Fermilab/MILC lattice data [22]:

$$h_{A_1}(1) = 0.906 \pm 0.013\,. \tag{2.1}$$

In addition to these, we have used, in few cases, the inputs from light cone sum rule (LCSR) [23]:

$$h_{A_1}(w_{max}) = 0.65(18), \quad R_1(w_{max}) = 1.32(4), \quad R_2(w_{max}) = 0.91(17), \tag{2.2}$$

and the following inputs throughout our analysis:

$$\begin{aligned} \bar{m}_b(\bar{m}_b) = 4.163 \pm 0.016\ GeV,\ m_c(3GeV) = 0.986 \pm 0.013\ GeV, \\ \alpha_S(\bar{m}_b(\bar{m}_b)) = 0.2268 \pm 0.0023. \end{aligned} \tag{2.3}$$

## 3 CLN parameterization : Fit results

| Constraints | $\lvert V_{cb}\rvert$ ($\times 10^3$) | $\chi^2_{min}/d.o.f$ | $p$-value (%) | $R(D)$ |
|---|---|---|---|---|
| Using only $\mathcal{G}(1)$ | | | | |
| **HPQCD+MILC** | **39.97(1.34)** | **23.04/39** | **98.02** | **0.299(6)** |
| **HPQCD+MILC+BPS** | **40.04(1.33)** | **23.42/40** | **98.30** | **0.299(6)** |
| Belle [18] | 39.86(1.33) | 4.57/8 | 80 | 0.298(6) |
| Using only $f_+(w)$ | | | | |
| **HPQCD + MILC** | **40.84(1.15)** | **31.22/43** | **90.91** | **0.305(3)** |

**Table 3**: Result of the fit to the experimental data in $B \to D\ell\nu_\ell$ using only $\mathcal{G}(1)$ (first two rows), and using $f_+(w)$ ($w = 1$ and $w \neq 1$) from lattice (MILC and HPQCD listed in table 1) with the CLN parametrization of the form factors.

### 3.1 Fit from $B \to D\ell\nu_\ell$ data

As shown in Table 3, when we fit the available data using CLN parameterization for the form factors, we use different combinations of the predicted values of $\mathcal{G}(1)$. The best results are obtained when all the inputs are combined together, and the corresponding extracted

values of $|V_{cb}|$ and $R(D)$ are shown in table 3. To do a preliminary cross-check of the validity of the fits, we have completely reproduced the table (V) of ref. [18], except the last column, where the authors quote the fit results after averaging the separate samples. We have instead used the whole 40-data-point-long sample with the full correlation matrix and have considered values of $m_e$ and $m_\mu$ to incorporate the correct values of $w_{max}$ consistent with experimental results. The reason for doing this is two-fold: (a) The increased number of degrees of freedom improves the quality of fit considerably. Even with $d.o.f$ increased by a factor of 5, $\chi^2_{min}/d.o.f$ hardly increases. However, as can be seen from the $p$-values for our results in table 3, there is a considerable improvement in the goodness-of-fit. (b) We wanted to use the full correlation in the data. The fact that our results match with Belle for all sub-samples separately up to the second decimal place, while the full fit very slightly differs from the averaged result, makes the importance of considering the correlations even more pertinent. Using $\mathcal{G}(1)$ from HPQCD and MILC with or without the constraint from BPS gives us our obtained result, given in bold-faced font. For a comparison, in the third row of table 3, we quote the experimental results too. The experimental analysis fits the quantity $\eta_{EW}\mathcal{G}(1)|V_{cb}|$ and then uses the MILC value of $\mathcal{G}(1)$ and the electroweak correction factor $\eta_{EW} = 1.0066$ to calculate $|V_{cb}|$. We note a little increase in the central values of our estimates of $|V_{cb}|$ with respect to that of Belle, however, the percentage error in the estimate does not change. Also, as we have fitted $\mathcal{G}(1)$ separately under the above-mentioned constraints, it has a non-zero correlation with $|V_{cb}|$. With the increased number of data points, we obtain a better fit than [18], as can be seen from the $p$-values. The extracted values of $R(D)$ are also consistent with that extracted in [18].

The last row of the same table represents the results obtained from a fit to the available experimental data along with the lattice inputs on $f_+(w)$ (table 1). We note that the central value of the fitted $V_{cb}$ is increased by $\approx 2\%$ while the percentage error has reduced from 3.3% to 2.8%. Also, now we can compare the predicted values of $R(D)$, which are obtained from the fit with and without the lattice inputs on $f_+(w)$. The central value of the predicted $R(D)$ has increased due to the use of $f_+(w)$, and there is a considerable reduction in the percentage error of the estimate. Our result is in agreement with the prediction of the earlier analysis [11]. In our fit, we do not include the inputs on $f_0(w)$ from lattice, inclusion of which makes the fit worse (with a p-value $< 1\%$). However, the fit is not that bad (p-value $\approx 55\%$) if we drop all the available inputs from MILC and just use the inputs from HPQCD along with the experimantal data.

### 3.2 Fit from $B \to D^*\ell\nu_\ell$ data

For the decay $B \to D^*\ell\nu_\ell$ , details of the parametrization of the form factors can be seen in refs. [5, 10]. In addition to $|V_{cb}|$, there are 4 other parameters to fit in this case, of which $h_{A_1}(1)$ is put into the fit as a nuisance parameter with input from eq. (2.1). Fit results are listed in table 4. $|V_{cb}|$ obtained from this fit has slightly larger uncertainty than that has been obtained from the $B \to D\ell\nu_\ell$ fit, although there is a small decrease in the central value. The overall multiplicative parameter here is $h_{A_1}(1)|V_{cb}|$, so $h_{A_1}(1)$ has a correlation with $|V_{cb}|$ in our fit. Our fit values agree with those obtained in earlier analyses [7, 8], and

| | Data+Lattice | Data+Lattice+LCSR |
|---|---|---|
| Parameters/ Observables | Best Fit ± Err. Values | Best Fit ± Err. Values |
| $\boldsymbol{\|V_{cb}\| \times 10^3}$ | $\mathbf{38.23 \pm 1.46}$ | $\mathbf{38.15 \pm 1.43}$ |
| $\rho^2_{D^*}$ | $1.17 \pm 0.15$ | $1.16 \pm 0.14$ |
| $R_1(1)$ | $1.39 \pm 0.09$ | $1.37 \pm 0.04$ |
| $R_2(1)$ | $0.91 \pm 0.08$ | $0.91 \pm 0.07$ |
| $h_{A_1}(1)$ | $0.91 \pm 0.01$ | $0.91 \pm 0.01$ |
| $\chi^2_{min}$ | 34.14 | 34.62 |
| dof | 36 | 39 |
| $p$-value | 55.73% | 69.10% |
| $R_0(1)$ | $1.191 \pm 0.017$ | $1.195 \pm 0.017$ |
| $\boldsymbol{R(D^*)}$ | $\mathbf{0.255 \pm 0.004}$ | $\mathbf{0.255 \pm 0.004}$ |

**Table 4**: Fit results with CLN for $B \to D^* \ell \nu_\ell$ , combined with constraint from eq. (2.1)

| | Data+Lattice | Data+Lattice+LCSR |
|---|---|---|
| Parameters | Best Fit ± Err. Values | Best Fit ± Err. Values |
| $\boldsymbol{\|V_{cb}\| \times 10^3}$ | $\mathbf{39.82 \pm 0.90}$ | $\mathbf{39.77 \pm 0.89}$ |
| $\rho^2_D$ | $1.138 \pm 0.023$ | $1.138 \pm 0.023$ |
| $\mathcal{G}(1)$ | $1.058 \pm 0.007$ | $1.058 \pm 0.007$ |
| $\rho^2_{D^*}$ | $1.269 \pm 0.123$ | $1.251 \pm 0.113$ |
| $R_1(1)$ | $1.386 \pm 0.087$ | $1.371 \pm 0.036$ |
| $R_2(1)$ | $0.880 \pm 0.073$ | $0.888 \pm 0.065$ |
| $h_{A1}(1)$ | $0.900 \pm 0.012$ | $0.900 \pm 0.012$ |
| $\chi^2_{min}$ | 67.34 | 67.99 |
| dof | 79 | 82 |
| $p$-value | 82.21% | 86.66% |

**Table 5**: Results of the combined fit to the data in $B \to D^{(*)} \ell \nu_\ell$ with CLN.

in [19] [1]. Results obtained from a similar kind of fit, where, in addition to lattice, inputs from LCSR (eq. 2.2) have been incorporated, are shown in the right panel of table 4. We note that although there are no considerable changes in the fitted values of $|V_{cb}|$, the error in the extracted value of $R_1(1)$ has reduced from 6.5% to 3%. The uncertainties in all the other fit parameters have reduced (though not considerably).

The calculation of $R(D)$ in CLN parametrization is straightforward. However, as mentioned earlier, calculation of $R(D^*)$ depends on an additional form factor ratio $R_0(w)$ and its value calculated at zero-recoil, which can not be fitted from $B \to D^* \ell \nu_\ell$. The form

[1] The preprint of a parallel work shares a similar publication timeline with our work.

| Cases | Inputs for the fits |
|---|---|
| case-1 | $R_1(1)$, $R_2(1)$, $f_+(w)/f_0(w)$ for $w$=1, 1.08, 1.16 (MILC) and $w$= 1.03, 1.06, 1.09, 1.12 (HPQCD) |
| case-2 | case-1 with $R_1(w_{max})$, $R_2(w_{max})$ from LCSR. |

**Table 6**: Different cases for the fit of sub-leading Isgur-Wise functions.

factor ratios $R_i(w)$s are expressed as the ratios of the HQET form factors [5, 14] $h_i$s, like

$$R_1(w) = \frac{h_v}{h_{A_1}}, \qquad R_2(w) = \frac{h_{A_3}}{h_{A_1}} + r_{D^*}\frac{h_{A_2}}{h_{A_1}},$$
$$R_0(w) = \frac{(w+1)}{(1+r_{D^*})} - \frac{(w-r_{D^*})}{(1+r_{D^*})}\frac{h_{A_3}}{h_{A_1}} - \frac{(1-wr_{D^*})}{(1+r_{D^*})}\frac{h_{A_2}}{h_{A_1}}, \tag{3.1}$$

where $r_{D^*} = m_{D^*}/m_B$. The $h_i$s, and hence the form factor ratios include the corrections at order $\alpha_s$ and $\Lambda_{QCD}/m_{b,c}$. They are expressed in terms of a few sub-leading Isgur-Wise functions (HQET parameters), like $\eta(1), \eta'(1), \chi_2(1), \chi_2'(1)$, and $\chi_3'(1)$. We note that both $R_2(w)$ and $R_0(w)$ are sensitive to the ratios $h_{A_3}/h_{A_1}$ and $h_{A_2}/h_{A_1}$. In the HQET, the $R_1(1)$, $R_2(1)$ and $R_0(1)$ are obtained from eq. 3.1 by taking the limit $w \to 1$, and all of them are functions of the above mentioned HQET parameters. Hence, the $R_0(1)$ can be estimated only after the extractions of these HQET parameters.

Also, the form factor ratios $f_+(w)/f_0(w)$ can be expressed in terms of the ratios of the HQET form factors, like

$$\frac{f_+(w)}{f_0(w)} = \frac{(1+r_D)^2}{2r_D(w+1)}\left(\frac{\frac{h_-}{h_+}\frac{1-r_D}{1+r_D} - 1}{\frac{h_-}{h_+}\frac{1+r_D}{1-r_D}\frac{w-1}{w+1} - 1}\right), \tag{3.2}$$

with $r_D = m_D/m_B$. The HQET form factors $h_+$ and $h_-$ are also known at order $\alpha_s$ and $\Lambda_{QCD}/m_{b,c}$, and can be expressed in terms of the above mentioned five HQET parameters.

In the CLN parameterization of the form factors, we have expressed $R_i(w)$ as given in eq. (B7) of ref. [10] and fit $R_2(1)$ and $R_1(1)$ from the available data. Using these fit results and the inputs from lattice, we then estimate $R_0(1)$ after extracting the HQET parameters for the cases mentioned in table 6. The predictions of $R(D^*)$ in both the cases are shown in table 4.

### 3.3 Combined fit from $B \to D\ell\nu_\ell$ and $B \to D^*\ell\nu_\ell$ data:

Combining the full set of $w$-binned data from all subsamples for $B \to D\ell\nu_\ell$ and the full data-set with all four variables for $B \to D^*\ell\nu_\ell$ gives us the unique opportunity to not only simultaneously fit all the form factor parameters along with $|V_{cb}|$, but also predict the values and correlated uncertainties of $R(D)$ and $R(D^*)$ together. The fit results are listed in table 5. The combined fit of the data in $B \to D\ell\nu_\ell$ and $B \to D^*\ell\nu_\ell$ shows considerable improvement over that obtained from the analysis of only the decay $B \to D^*\ell\nu_\ell$ . Though changes in the fitted values of $R_1(1)$ and $R_2(1)$ are small, extracted uncertainties of $|V_{cb}|$ reduces to $\approx 2\%$ and the central value of $\rho^2_{D^*}$ increases by approximately 8% in the combined

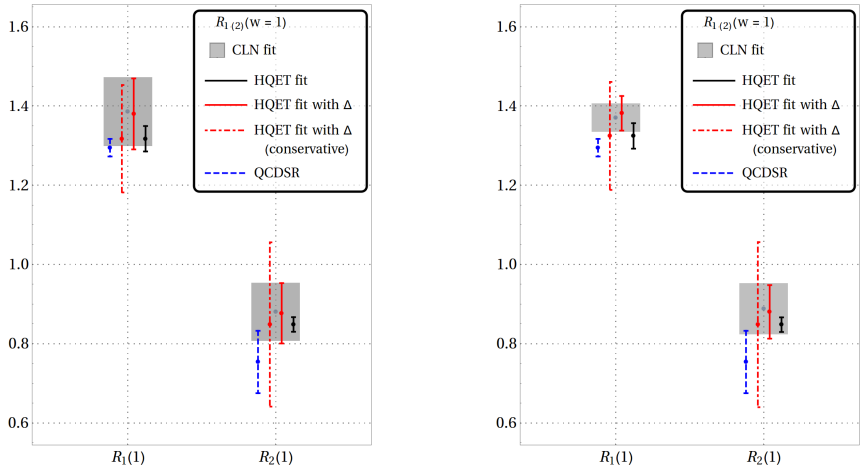



**Figure 1**: Comparisions between different $R_1(1)$ and $R_2(1)$ which are obtained from different fits, with (right) and without (left) the inputs from LCSR, and QCDSR. For the conservative estimates of $R_{1(2)}(w=1)$, $\Delta_v$ is taken as $1 \pm 0.1$ and each of $\Delta_{21}$ and $\Delta_{31}$ is considered as $1 \pm 0.2$.

| Parameters | case-1 | case-1 with Δs | case-2 | case-2 with Δs |
|---|---|---|---|---|
| $\eta(1)$ | 0.39(3) | 0.40(5) | 0.39(3) | 0.40(5) |
| $\eta'(1)$ | -0.002(100) | 0.004(101) | -0.03(9) | 0.001(101) |
| $\chi_2(1)$ | -0.08(1) | -0.06(1) | -0.08(1) | -0.06(1) |
| $\chi_2'(1)$ | -0.003(2) | -0.003(2) | -0.001(2) | -0.002(2) |
| $\chi_3'(1)$ | 0.04(2) | 0.04(2) | 0.05(2) | 0.04(2) |
| $\Delta_v$ | - | 1.05(6) | - | 1.05(2) |
| $\Delta_{21}$ | - | 1.00(20) | - | 1.00(20) |
| $\Delta_{31}$ | - | 1.04(8) | - | 1.04(7) |
| $\Delta_{\mp}$ | | 1.00(20) | - | 1.00(20) |
| $\chi^2_{min}$ | 4.34 | 3.36 | 9.20 | 3.62 |
| dof | 7 | 7 | 9 | 9 |
| $p$-value | 73.95% | 85.00% | 41.90% | 93.46% |

**Table 7**: The fit results for the subleading Isgur-Wise functions and the Δs (see text).

analysis. Using the fit results given in table 5 and the inputs from lattice and LCSR, we obtain $R_0(1)$ and hence $R(D^*)$ for the cases given in table 6. For details, see 2nd (case-1) and 4th (case-2) columns of table 8. Also in the combined analysis of all datasets, the central values of the predicted $R(D^*)$ increase by approximately 2%, and the uncertainties are about 1%.

| Parameters/ Observables | case-1 | case-1 with $\Delta_{31}$ & $\Delta_{21}$ = 1.00(20) | case-2 | case-2 with $\Delta_{31}$ & $\Delta_{21}$ = 1.00(20) |
|---|---|---|---|---|
| $R_0(1)$ | 1.192(17) | 1.192(101) | 1.196(17) | 1.196(102) |
| $\boldsymbol{R(D)}$ | **0.304(3)** | **0.304(3)** | **0.304(3)** | **0.304(3)** |
| $\boldsymbol{R(D^*)}$ | **0.259(3)** | **0.259(6)** | **0.259(3)** | **0.259(6)** |
| Corr($R(D)$ -$R(D^*)$) | 0.21 | 0.12 | 0.20 | 0.11 |

**Table 8**: The SM predictions for $R(D)$ and $R(D^*)$.

### 3.3.1 $R(D^*)$ with the additional error $\Delta$

For completeness, as was mentioned in the introduction, we have also introduced additional parameters ($\Delta$), which parametrize the unknown higher order corrections in the ratios of the HQET form factors, such as $h_v/h_{A_1}$, $h_{A_3}/h_{A_1}$, $h_{A_2}/h_{A_1}$ and $h_-/h_+$. In order to estimate the probable size of those missing corrections, we have made the following replacements in eqs. 3.1 and 3.2:

$$\frac{h_v}{h_{A_1}} \to \frac{h_v}{h_{A_1}}\Delta_v, \quad \frac{h_{A_3}}{h_{A_1}} \to \frac{h_{A_3}}{h_{A_1}}\Delta_{31}, \quad \frac{h_{A_2}}{h_{A_1}} \to \frac{h_{A_2}}{h_{A_1}}\Delta_{21}, \quad \frac{h_-}{h_+} \to \frac{h_-}{h_+}\Delta_{\mp}. \tag{3.3}$$

Though these $\Delta$s could be $w$ dependent in general, for values of $w$ very close to 1, these dependencies can be neglected. Thus we assume these $\Delta$s to be $w$ independent for simplicity. Following the above-mentioned methods, we then fit these additional parameters along with the HQET sub-leading Isgur-Wise functions using all the available datasets as mentioned in table 6, with a goal to find out the size of these newly introduced parameters. In our analysis, $\Delta$s are treated as normally distributed nuisance parameters with $\Delta = 1.0 \pm 0.2$, i.e. we have allowed these missing corrections to vary at most by 20%.

Table 7 (3rd and 5th column) shows the fit results of the HQET parameters and the $\Delta$s with the corresponding $1\sigma$ errors, for the scenarios listed in table 6. We note that $\Delta_{\mp}$ and $\Delta_{21}$ could be as large as 20%, while $\Delta_v$ and $\Delta_{31}$ are $< 15\%$. The set of parameter values thus obtained is used to estimate the best-fit values and uncertainties in $R_1(1)$ and $R_2(1)$. In figure 1, these fitted results for $R_{1(2)}(1)$ are compared with those obtained previously from the CLN fit and with the QCDSR predictions. Our CLN fit results of $R_1(1)$ and $R_2(1)$ have large uncertainties, and are marginally consistent with the QCDSR predictions, whereas those obtained using our fit results for the HQET parameters without $\Delta$s (i.e. cases 1 and 2 of 7) have small errors (shown as solid black bars) and lie in between the CLN fit results and QCDSR predictions. In the same plot, the solid red bars represent the best fit values and the error bars of $R_1(1)$ and $R_2(1)$, which are obtained using the parameter values of the $\Delta_v$, $\Delta_{21}$, and $\Delta_{31}$ and the other HQET parameters as given in table 7. With these sets of parameters, we can now fully reproduce the CLN fit results, and hence, will

be marginally consistent with the QCDSR predictions. However, if we take $\Delta_v = 1 \pm 0.1$, $\Delta_{21} = 1 \pm 0.2$, and $\Delta_{31} = 1 \pm 0.2$ (conservative estimates[2]) then we can fully reproduce the CLN fit results, as well as the QCDSR predictions; the results are shown as dot-dashed red bars in figure 1. Using the results given in table 7, we estimate $R_0(1)$ for the above mentioned different cases. With these $R_0(1)$s and the CLN fit results given in table 5, we obtain $R(D^*)$ which are presented in table 8. The errors in the estimated $R(D^*)$ have increased from 1.16% to 2.32% due to introduction of an additional error of about 20% in the HQET form factor ratios.

## 4 BGL parametrization

### 4.1 Formalism and Results for $|V_{cb}|$

| Data+Lattice (HPQCD & MILC) | | | |
|---|---|---|---|
| Parameters/ Observables | Best Fit Values | ± Err | Err. from $\Delta\chi^2 = \pm 1$ |
| $\lvert V_{cb}\rvert \times 10^3$ | 41.04 | 1.13 | $\left(^{+1.12}_{-1.13}\right)$ |
| $a_0^{f+}$ | 0.0141 | 0.0001 | (0.0001) |
| $a_1^{f+}$ | -0.0318 | 0.0028 | (0.0028) |
| $a_2^{f+}$ | -0.0819 | 0.0199 | (0.0199) |
| $a_1^{f0}$ | -0.1961 | 0.0136 | (0.0136) |
| $a_2^{f0}$ | -0.2274 | 0.0942 | (0.0942) |
| $\chi^2_{min}$ | 33.37 | | |
| dof | 46 | | |
| $p$-value | 91.77% | | |
| R(D) | 0.302 ±0.003 | | |

**Table 9**: The fit results obtained from the analysis of the decay $B \to D\ell\nu_\ell$ with the BGL parameterization of the form factors for $N = 2$.

The BGL parameterization of the form factors rely on a Taylor series expansion about $z = 0$. The key ingredient in this approach is the transformation that maps the complex $q^2$ [3] plane onto the unit disc $|z| \leq 1$. The most general form of the expansion of the form factors is given as [6]

$$F_i(z) = \frac{1}{P_i(z)\phi_i(z)} \sum_{n=0}^{N} a_n^{\mathcal{F}_i}\ z^n, \tag{4.1}$$

where

$$z = \frac{\sqrt{w+1} - \sqrt{2}}{\sqrt{w+1} + \sqrt{2}}. \tag{4.2}$$

[2]Here, we have used the maximum attainable values of the $\Delta$s, which are allowed by the data. From the fit, the allowed values of $\Delta_{31}$ is $< 15\%$, however, for the conservative estimates we have allowed it to be as large as 20%.

[3]In our case, $q^2 = (p_\ell + p_\nu)^2$

| Parameters | Data+Lattice | | Data+Lattice+LCSR | |
|---|---|---|---|---|
| | Best Fit Values | Err. from $\Delta\chi^2 = 1$ | Best Fit Values | Err. from $\Delta\chi^2 = 1$ |
| $\lvert V_{cb}\rvert \times 10^3$ | 41.7 | $\binom{+2.0}{-2.1}$ | 40.6 | (1.7) |
| $a_0^f$ | 0.0109 | (0.0002) | 0.0109 | (0.0002) |
| $a_1^f$ | -0.0459 | $\binom{+0.0527}{-0.0429}$ | -0.0518 | $\binom{+0.0267}{-0.0131}$ |
| $a_2^f$ | 0.1513 | $\binom{0.8457}{-1.1508}$ | 0.9942 | $\binom{+0.0047}{-0.5019}$ |
| $a_1^{\mathcal{F}_1}$ | -0.0092 | $\binom{+0.0054}{-0.0050}$ | -0.0070 | $\binom{+0.0048}{-0.0046}$ |
| $a_2^{\mathcal{F}_1}$ | 0.1150 | $\binom{+0.0877}{-0.0921}$ | 0.0932 | $\binom{+0.0850}{-0.0883}$ |
| $a_0^g$ | 0.0111 | $\binom{+0.0104}{-0.0075}$ | 0.0257 | $\binom{+0.0054}{-0.0034}$ |
| $a_1^g$ | 0.5786 | $\binom{+0.3351}{-0.4007}$ | 0.0836 | $\binom{+0.0753}{-0.2157}$ |
| $a_2^g$ | 0.8155 | $\binom{+0.1683}{-1.7701}$ | -0.9962 | $\binom{+1.9958}{-0.0036}$ |
| $\chi^2_{min}$ | 27.81 | | 30.93 | |
| dof | 32 | | 35 | |
| $p$-value | 67.87% | | 66.51% | |

**Table 10**: Fit results with BGL parameterization of the form factors ($N = 2$) in $B \to D^*\ell\nu_\ell$ .

Here, $F_i(z)$ include $f_+(z)$, $f_0(z)$, associated with the decays $B \to D$, and those associated with $B \to D^*$ are given by $F_1(z)$, $f(z)$, $g(z)$ and $F_2(z)$ respectively. The coefficients $a_n^{\mathcal{F}_i}$ follow weak as well as strong unitarity constraints [6]. However, along the lines of ref.s [6, 7, 11], we have used the weak unitarity constraints for the coefficients $a_n^{f_+}$, $a_n^{f_0}$, $a_n^{\mathcal{F}_1}$, $a_n^f$, $a_n^g$ and $a_n^{\mathcal{F}_2}$, and considered the form factors with $N = 2$ in our analysis. The weighting functions $\phi_i(z)$ contain the Jacobian of the variable transformation and the physics of the perturbative QCD (PQCD). It is also analytic on the unit disc. The mathematical forms of these $\phi_i$'s, corresponding to various spin states, can be seen from [6]. Another important ingredient in this form of parameterization is the Blaschke factor, which is defined as

$$P(z) = \prod_p \frac{z - z_p}{1 - z z_p}, \tag{4.3}$$

where

$$z_p = \frac{\sqrt{t_+ - m_p^2} - \sqrt{t_+ - t_0}}{\sqrt{t_+ - m_p^2} + \sqrt{t_+ - t_0}}, \tag{4.4}$$

with

$$t_+ = (m_B + m_{D^{(*)}})^2, t_- = (m_B - m_{D^{(*)}})^2, t_0 = t_- \tag{4.5}$$

Here, $z = z_p$ represents the location of a pole i.e $B_c$ narrow resonance. The $P(z)$ is analytic on the unit disc for $|z_p| \leq 1$. In general, the form factors $F_i(q^2)$ have poles, and the Blaschke factor is useful to eliminate those poles of $F_i$'s at $z = z_p$, such that $P_i F_i$ is analytic on the unit disc $|z| \leq 1$.

In our analysis, the various inputs relevant to the BGL parameterization of the form factors associated with the decays $B \to D\ell\nu_\ell$ and $B \to D^*\ell\nu_\ell$ ($\ell = \mu$ and e) are taken from

| Parameters | Data+Lattice | | Data+Lattice+LCSR | |
|---|---|---|---|---|
| | Best Fit Values | Err. from $\Delta\chi^2 = 1$ | Best Fit Values | Err. from $\Delta\chi^2 = 1$ |
| $\lvert V_{cb}\rvert \times 10^3$ | 41.2 | (1.0) | 40.9 | (0.9) |
| $a_0^f$ | 0.0109 | (0.0002) | 0.0109 | (0.0001) |
| $a_1^f$ | -0.0366 | $\binom{+0.0409}{-0.0422}$ | -0.0534 | $\binom{+0.0194}{-0.0112}$ |
| $a_2^f$ | -0.0340 | $\binom{+1.0312}{-0.9652}$ | 0.9936 | $\binom{+0.0049}{-0.4022}$ |
| $a_1^{\mathcal{F}_1}$ | -0.0084 | $\binom{+0.0045}{-0.0044}$ | -0.0074 | $\binom{+0.0043}{-0.0042}$ |
| $a_2^{\mathcal{F}_1}$ | 0.1054 | $\binom{+0.0846}{-0.0855}$ | 0.0983 | $\binom{+0.0821}{-0.0830}$ |
| $a_0^g$ | 0.0112 | $\binom{+0.0108}{-0.0075}$ | 0.0256 | $\binom{+0.0052}{-0.0033}$ |
| $a_1^g$ | 0.5882 | $\binom{+0.3320}{-0.4233}$ | 0.0800 | $\binom{+0.0722}{-0.2131}$ |
| $a_2^g$ | 0.8038 | $\binom{+0.1783}{-1.7582}$ | -0.9925 | $\binom{+1.9887}{-0.0038}$ |
| $a_0^{f_+}$ | 0.0141 | (0.0001) | 0.0141 | (0.0001) |
| $a_1^{f_+}$ | -0.0320 | (0.0027) | -0.0317 | (0.0027) |
| $a_2^{f_+}$ | -0.0816 | (0.0199) | -0.0822 | (0.0198) |
| $a_1^{f_0}$ | -0.1967 | (0.0134) | -0.1956 | (0.0134) |
| $a_2^{f_0}$ | -0.2291 | (0.0941) | -0.2259 | (0.0940) |
| $\chi^2_{min}$ | 61.26 | | 64.35 | |
| dof | 79 | | 82 | |
| $p$-value | 93.04% | | 88.35% | |

**Table 11**: The fit results obtained from the combined analysis of the available data in the decays $B \to D\ell\nu_\ell$ and $B \to D^*\ell\nu_\ell$ with the BGL parameterization of the form factors with $N = 2$.

the references [6, 7, 11]. The fit results are shown in Tables 9 and 10 respectively. The results of the combined analysis of data in $B \to D^{(*)}\ell\nu_\ell$ are shown in Table 11. In the combined analysis, we use the following weak unitarity constraints:

$$\begin{aligned}(a_0^g)^2 + (a_1^g)^2 + (a_2^g)^2 + (a_0^{f_+})^2 + (a_1^{f_+})^2 + (a_2^{f_+})^2 < 1,\\ (a_0^{\mathcal{F}_1})^2 + (a_1^{\mathcal{F}_1})^2 + (a_2^{\mathcal{F}_1})^2 + (a_0^f)^2 + (a_1^f)^2 + (a_2^f)^2 < 1,\\ (a_0^{f_0})^2 + (a_1^{f_0})^2 + (a_2^{f_0})^2 < 1.\end{aligned} \tag{4.6}$$

We note that the uncertainties of the extracted $|V_{cb}|$ have reduced to $\approx 2\%$. This is the most precise estimate obtained so far from a combined analysis. In addition, we observe that the central values of the $|V_{cb}|$ obtained from BGL analysis is increased by approximately 3.5% for combined fit without LCSR and 3% for combined fit with LCSR than those obtained using the CLN parameterizations for the form factors.

### 4.2 Predictions for $R(D^{(*)})$

As mentioned earlier, the decay $B \to D^*\tau\nu_\tau$ is sensitive to an additional form factor [6]

$$F_2(z) = \frac{1}{P_2(z)\phi_2(z)} \sum_{n=0}^{N} a_n^{\mathcal{F}_2}\ z^n \tag{4.7}$$

with

$$P_2(z) = \prod_{p=1}^{3} \frac{z - z_p}{1 - z z_p}, \tag{4.8}$$

and

$$\phi_2(z) = \sqrt{\frac{2n_I}{\pi \tilde{\chi}_{0^-}}} \frac{2^3 (r)^2 (1+z)^2 (1-z)^{-\frac{1}{2}}}{[(1+r)(1-z) + 2\sqrt{r}(1+z)]^4}. \tag{4.9}$$

Here, $n_I$ represents the number of light valence quarks or the effective iso-spin factor, as given in [11]. We use $n_I = 2.6$. The functions $\tilde{\chi}_{0^-}$ are defined as [5]

$$\tilde{\chi}_{0^-}(0) = \chi_{0^-}(0) - \sum_{n=1} \frac{f_n^2(B_c)}{M_n^2(B_c)}, \tag{4.10}$$

where $\chi_{0^-}(0)$ are the perturbatively calculable functions and associated with the once-subtracted QCD dispersion relation ( for details see [6]). The second term represents the contribution to the dispersion relations from the $0^-$ $B_c$-type resonances below the $BD^*$ type pair production. The decay widths and masses of those resonances are given by $f_n$ and $M_n$ respectively, and their respective values are given in Table 12.

| Form-factor | Resonance type | Mass, $M_n$ in GeV | Decay constant, $f_n$ in GeV |
|---|---|---|---|
| $F_2$ | $0^-$ | 6.275 | 0.427 |
| | | 6.842 | |
| | | 7.250 | |

**Table 12**: The decay widths and the masses of the $B_c$ resonances.

Expressions of $\chi_{0^-}(0)$ include the corrections at order $\alpha_s$. We obtain $\chi_{0^-} = (1.807 \pm 0.009) \times 10^{-2}$ using the inputs given in eq. 2.3. However, incorporating the corrections of order $\alpha_s^2$, one will obtain $\chi_{0^-} = 1.942 \times 10^{-2}$ [19].

In eq. 4.7, the unknowns are the various coefficients $a_n^{\mathcal{F}_2}$. For $N = 2$ these are, respectively, $a_0^{\mathcal{F}_2}$, $a_1^{\mathcal{F}_2}$ and $a_2^{\mathcal{F}_2}$. Hence, in order to predict $R(D^*)$ one needs to extract these coefficients, and HQET relations between the form factors are very useful in this regard. In order to extract these coefficients, we use the following equations

$$F_2(w) = \left(\frac{F_2(w)}{F_i(w)}\right)_{HQET} F_i(w), \quad i \neq 2. \tag{4.11}$$

Here, $F_i(w)$'s can be anyone of $f_+(w)$, $f_0(w)$, $F_1(w)$ and $f(w)$. As mentioned earlier, the HQET form factors at order $\alpha_s$ and $\Lambda_{QCD}/m_{b,c}$ are given in terms of the five HQET parameters (for details see [14]). For the known values of these parameters, the r.h.s of eq. 4.11 are different numbers for different values of $w$ ($\geq 1$), since $F_i(w)$ are known, either from our fits or from the lattice. Hence, we can create synthetic data points for $F_2(w)$ for different values of $w$.

| Cases | Inputs for the fits |
|---|---|
| case-3 | $F_1(w)/f(w)$ for $w$=1.03, 1.06, 1.09 and $f_+(w)/f_0(w)$ for $w$=1, 1.03, 1.06, 1.09 from BGL fit results (table 11) |
| case-4 | case-3 with $R_1(w_{max})$ and $R_2(w_{max})$ from LCSR |
| case-5 | $f_+(w)/f_0(w)$ for $w$=1, 1.08, 1.16 (MILC) and $w$=1.03, 1.06, 1.09, 1.12 (HPQCD) |
| case-6 | case-5 with $R_1(w_{max})$ and $R_2(w_{max})$ from LCSR |

**Table 13**: Different cases for the fit of sub-leading Isgur-Wise functions.

| Parameters | case-3 | case-3 with $\Delta$s | case-4 | case-4 with $\Delta$s | case-5 | case-5 with $\Delta$s | case-6 | case-6 with $\Delta$s |
|---|---|---|---|---|---|---|---|---|
| $\eta(1)$ | 0.39(3) | 0.39(5) | 0.38(3) | 0.40(5) | 0.39(4) | 0.40(5) | 0.40(3) | 0.40(5) |
| $\eta'(1)$ | 0.10(7) | 0.12(5) | 0.08(7) | 0.14(7) | 0.01(12) | 0.004(101) | -0.02(10) | 0.003(101) |
| $\chi_2(1)$ | -0.07(6) | -0.05(6) | -0.11(5) | -0.08(6) | -0.06(6) | -0.06(6) | -0.06(6) | -0.06(6) |
| $\chi_2{}'(1)$ | 0.007(60) | -0.02(4) | 0.006(59) | -0.004(30) | -0.003(60) | -0.003(60) | -0.002(59) | -0.003(60) |
| $\chi_3{}'(1)$ | 0.06(5) | 0.06(4) | 0.06(5) | 0.04(4) | 0.04(6) | 0.04(6) | 0.05(6) | 0.04(6) |
| $\Delta_v$ | - | - | - | 1.06(3) | - | - | - | 1.06(3) |
| $\Delta_\mp$ | - | 0.98(20) | - | 1.00(20) | - | 1.00(20) | - | 1.00(20) |
| $\Delta_{21}$ | - | 1.05(20) | - | 1.02(20) | - | - | - | 1.00(20)) |
| $\Delta_{31}$ | - | 1.03(10) | - | 1.07(7) | - | - | - | 1.01(13) |
| $\chi^2_{min}$ | 1.71 | 1.73 | 7.63 | 1.88 | 3.84 | 3.26 | 7.05 | 3.36 |
| dof | 5 | 5 | 7 | 7 | 5 | 5 | 7 | 7 |
| $p$-value | 88.77% | 88.54% | 36.62% | 96.60% | 57.25% | 66.02% | 42.36% | 84.97% |

**Table 14**: The fit results for the subleading Isgur-Wise parameters with $\chi_2(1)$, $\chi_2'(1)$ and $\chi_3'(1)$ varied within their QCDSR 3 $\sigma$ range.

In the HQET, the form factor ratios $F_1(w)/f(w)$ and $F_2(w)/f(w)$ are given by

$$\begin{aligned}\frac{F_1(w)}{f(w)} &= m_B(w-1)\left(\frac{w-r_{D^*}}{w-1} - \frac{h_{A_2}}{h_{A_1}} r_{D^*} - \frac{h_{A_3}}{h_{A_1}}\right), \\ \frac{F_2(w)}{f(w)} &= \frac{1}{m_B r_{D^*}}\left(1 - \frac{h_{A_2}}{h_{A_1}}\frac{1-r_{D^*}w}{1+w} - \frac{h_{A_3}}{h_{A_1}}\frac{w-r_{D^*}}{1+w}\right).\end{aligned} \tag{4.12}$$

We can also define

$$\frac{F_2(w)}{F_1(w)} = \frac{F_2(w)}{f(w)}\frac{f(w)}{F_1(w)}, \tag{4.13}$$

such that all these form factor ratios are sensitive to $h_{A_2}/h_{A_1}$ and $h_{A_3}/h_{A_1}$. The other form

| Para-meters | case-3 | case-3 with $\Delta$s | case-4 | case-4 with $\Delta$s | case-5 | case-5 with $\Delta$s | case-6 | case-6 with $\Delta$s |
|---|---|---|---|---|---|---|---|---|
| $\eta(1)$ | 0.39(3) | 0.40(4) | 0.37(3) | 0.40(4) | 0.39(3) | 0.40(5) | 0.39(3) | 0.40(5) |
| $\eta'(1)$ | 0.13(4) | 0.13(4) | 0.11(4) | 0.14(4) | 0.005(105) | 0.003(92) | -0.02(10) | 0.002(92) |
| $\chi_2(1)$ | -0.06(2) | -0.06(2) | -0.07(2) | -0.06(2) | -0.06(2) | -0.06(2) | -0.06(2) | -0.06(2) |
| $\chi_2'(1)$ | 0.001(20) | -0.003(14) | 0.001(20) | -0.004(14) | -0.000(20) | -0.000(20) | -0.000(20) | -0.000(20) |
| $\chi_3'(1)$ | 0.04(2) | 0.04(2) | 0.04(2) | 0.04(2) | 0.04(2) | 0.04(2) | 0.04(2) | 0.04(2) |
| $\Delta_v$ | - | - | - | 1.06(3) | - | - | - | 1.06(3) |
| $\Delta_\mp$ | - | 1.00(19) | - | 0.98(19) | - | 1.00(20) | - | 1.00(20) |
| $\Delta_{21}$ | - | 1.00(20) | - | 0.98(20) | - | - | - | 1.00(20) |
| $\Delta_{31}$ | - | 1.03(10) | - | 1.08(6) | - | - | - | 1.01(13) |
| $\chi^2_{min}$ | 1.92 | 1.68 | 8.58 | 1.80 | 3.84 | 3.26 | 7.36 | 3.36 |
| dof | 5 | 5 | 7 | 7 | 5 | 5 | 7 | 7 |
| $p$-value | 85.97% | 89.07% | 28.39% | 97.02% | 57.19% | 65.96% | 39.26% | 84.94% |

**Table 15**: The fit results for the subleading Isgur-Wise parameters with $\chi_2(1)$, $\chi_2'(1)$ and $\chi_3'(1)$ varied within their QCDSR 1 $\sigma$ range.

factor ratios, which can also be used in the extractions of $R(D^*)$ are given by

$$\frac{F_2(w)}{f_+(w)} = 2\frac{\left(1+w-\frac{h_{A_2}}{h_{A_1}}(1-r_{D^*}w)+\frac{h_{A_3}}{h_{A_1}}(r_{D^*}-w)\right)}{\frac{\sqrt{r_{D^*}}}{\sqrt{r_D}}\frac{h_+}{h_{A_1}}(\frac{h_-}{h_+}(r_D-1)+(1+r_D))},$$
$$\frac{F_2(w)}{f_0(w)} = \frac{\left(1-\frac{h_{A_2}}{h_{A_1}}(1-r_{D^*}w)+\frac{h_{A_3}}{h_{A_1}}(r_{D^*}-w)\right)}{\frac{\sqrt{r_{D^*}}\sqrt{r_D}}{r_D+1}\frac{h_+}{h_{A_1}}(\frac{h_-}{h_+}\frac{(r_D+1)(w-1)}{(r_D-1)(w+1)}+1)}. \tag{4.14}$$

Apart from $h_{A_2}/h_{A_1}$ and $h_{A_3}/h_{A_1}$, these ratios are sensitive to $h_-/h_+$ and $h_+/h_{A_1}$.

Using the fit results given in table 11, we generate the synthetic data points for the ratios $F_1(w)/f(w)$ and $f_+(w)/f_0(w)$, for different values of $w(\geq 1)$. We first fit the subleading Isgur-Wise functions using those synthetic data points. In the analysis, the different benchmark cases are defined in table 13 and the respective fit results are shown in table 14. The lattice inputs are playing the major role in all the fits, and all the fits are good with physically plausible values for the HQET parameters. We note here that in general, the ratios of the form factors are more sensitive to $\eta(1)$ than the other HQET parameters. The values of the HQET parameters predicted in QCDSR have large errors ($\gtrsim 30\%$). For all of our intents and purposes, while taking the range of these parameters seriously, we do not regard their central values with similar import. Therefore, we had initially tried to fit all the HQET parameters from the data and lattice. In general, the fits were not good, and on top of that the error values of the parameters $\chi_2(1)$, $\chi_2'(1)$ and $\chi_3'(1)$ were very large, in some cases, the errors were almost eight times the corresponding best fit values. Also, the best fit values of these parameters were almost $\gtrsim 3\sigma$ away than the respective QCDSR

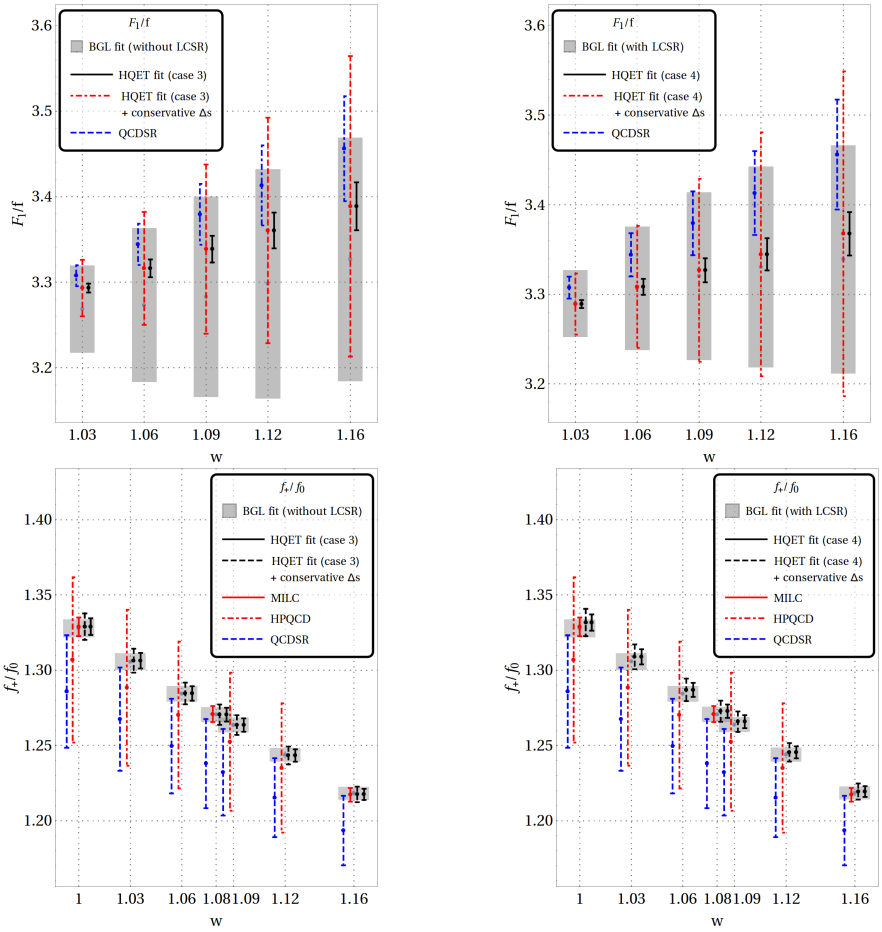



**Figure 2**: Upper half panel: Comparisons between different fit results of $F_1(w)/f(w)$ ($1\sigma$ bars) with (right) and without (left) the inputs from LCSR. Lower half panel: The ratio $f_+/f_0$ obtain from different fits, and from lattice. The fit results are also compared with the QCDSR predictions.

predictions. In all those fits, the parameter $\eta(1)$ had small errors. However, $\eta'(1)$ had large errors but it was in accordance with the QCDSR prediction.

Thus, in order to get a good fit of the data with reasonable and conservative uncertainties in the extracted parameters, we have considered $\chi_2(1)$, $\chi_2'(1)$ and $\chi_3'(1)$ as nuisance parameters, but varied them as gaussians in a broader range of three times the uncertainties associated with QCDSR predictions [14–16], which means our inputs for the fits are

$$\chi_2(1) = -0.06 \pm 0.06, \quad \chi_2'(1) = 0 \pm 0.06, \quad \chi_3'(1) = 0.04 \pm 0.06. \tag{4.15}$$

The corresponding results are given in table 14. For completeness, we have also provided the set of results with the parameters varied as a nuisance gaussian over their predicted QCDSR range, in table 15. The relaxed ranges of $\chi_2(1)$, $\chi_2'(1)$ and $\chi_3'(1)$ of the former fit normally produces larger uncertainties on the fitted parameters (table 14). This, while having virtually no effect on the $R(D^*)$ calculation (this fact can be checked by comparing

tables 16 and 17 ), increases the quality of the fits somewhat and we have used them in our analysis. In the upper half panel of the figure 2, various fit results of $F_1/f$ ($1\sigma$ bars) as well as the predictions from QCDSR for different values of $w$ are compared. The BGL fit results (table 11) have large uncertainties, while uncertainties obtained using the fitted HQET parameters (cases 3 and 4 from table 14) are very small. As can be understood from the lower-half panel of figure 2, the tight constraints on the HQET parameters are mainly coming from the lattice results, in particular from the MILC collaboration, on $f_+(w)/f_0(w)$. Apart from the high $w$ values, the BGL fit results of $F_1/f$ are fully consistent with that of QCDSR predictions. However, the same ratios obtained using the HQET fit parameters are marginally consistent with the QCDSR predictions.

We define a few more cases in addition to those given in table 13 where we have introduced additional parameters $\Delta_{\mp}$, $\Delta_{31}$, $\Delta_{21}$, and $\Delta_v$ as before. Note that we have not used $g(w)$ in the extraction of HQET parameters, as the uncertainties in the fitted values of $g(w)$ are large compared to other form factors. However, the parameter $\Delta_v$ will appear in the calculation while using $R_1(w_{max})$ as input. In order to fit these $\Delta$s along with the HQET parameters, we have to use synthetic data points on these form factors ratios. The fit results are shown in table 14, and the allowed values of the $\Delta$s are same as those obtained previously in the analysis of the CLN fit results along with the lattice (table 7). Upon incorporating these results in eqs. 4.12, we get the estimates of the probable size of the additional errors in $F_1/f$, $F_2/f$ and $F_2/F_1$. For the ratios $F_2(w)/f_{+/0}(w)$, we need to know the probable size of the additional error in $h_+/h_{A_1}$, which can be obtained from a comparison of lattice result of $f_0(1)/f(1)$ with that obtained from the HQET fit results or QCDSR. We find it to be approximately 10%, and assume it to be same for all other values of $w$. We propagate all these errors and estimate the overall size of the $\Delta$ in $F_2(w)/f_{+/0}(w)$. In order to be conservative in further analysis, we choose $\Delta_{31} = 1 \pm 0.2$ and $\Delta_{21} = 1 \pm 0.2$, and reproduce the ratios $F_1(w)/f(w)$ which are shown in the upper pannel of figure 2 by the dot-dashed red bars. As expected, we can now fully reproduce the QCDSR results and most parts of the BGL fit results.

After the extraction of the HQET parameters, we use eq. 4.11 to generate synthetic data points for $F_2(w)$ for different values of $w$ ($\geq 1$). In order to generate these synthetic data points one needs to find out $F_2(w)/F_i(w)$ for different values of $w$. As mentioned earlier, $F_i(w)$ could be anyone of $f(w)$, $F_1(w)$, and $f_{+/0}(w)$. The ratios $(F_2(w)/f(w))$ and $(F_2(w)/F_1(w))$ are less sensitive to the HQET parameters as compared to $(F_2(w)/f_{+/0}(w))$. Therefore, for case 3 (table 13), we have replaced $F_i(w)$ in eq. 4.11 by both $f(w)$ and $F_1(w)$ and created the above mentioned synthetic data points for $F_2(w)$. In case 4, the synthetic data points for $F_2(w)$ have been generated following the similar methods as are used in case 3. For completeness, we have replaced $F_i(w)$ by $f_+(w)$ and $f_0(w)$ for creating the synthetic data points in case 5, and the similar normalizations are used in case 6. These synthetic data points for $F_2(w)$ are used in eq. 4.7 to extract the coefficients $a_n^{\mathcal{F}_2}$ ( $n = 0, 1, 2$ ).

Once the synthetic data points are generated, in all the cases, the coefficient $a_0^{\mathcal{F}_2}$ can be extracted directly by solving eq. 4.7 for $w = 1$ or $z = 0$. Hence, the extracted values will be sensitive to $\eta(1)$ only. The extracted values of $a_0^{\mathcal{F}_2}$ which are shown in table 16 and

| Parameters/ Observables | $F_i(w)$ in eq. 4.11 : $F_1(w)$ & $f(w)$ | | $F_i(w)$ in eq. 4.11 : $F_1(w)$ & $f(w)$ | | $F_i(w)$ in eq. 4.11 : $f_+(w)$ & $f_0(w)$ | | $F_i(w)$ in eq. 4.11 : $f_+(w)$ & $f_0(w)$ | |
|---|---|---|---|---|---|---|---|---|
| | case-3 | case-3 with $\Delta$s | case-4 | case-4 with $\Delta$s | case-5 | case-5 with $\Delta$s | case-6 | case-6 with $\Delta$s |
| $a_0^{\mathcal{F}_2}$ | 0.053(1) | 0.053(4) | 0.053(1) | 0.053(5) | 0.058(1) | 0.058(8) | 0.058(1) | 0.058(8) |
| $a_2^{\mathcal{F}_2}$ | 0.21(6) | 0.21(8) | -0.14(3) | -0.17(10) | -0.48(1) | -0.42(2) | -0.39(1) | -0.33(1) |
| $R(D)$ | 0.302(3) | 0.302(3) | 0.302(3) | 0.302(3) | 0.302(3) | 0.302(3) | 0.302(3) | 0.302(3) |
| $\boldsymbol{R(D^*)}$ | **0.255(5)** | **0.255(5)** | **0.257(5)** | **0.257(5)** | **0.258(5)** | **0.258(7)** | **0.260(5)** | **0.260(7)** |
| Corr($R(D)$ -$R(D^*)$) | 0.12 | 0.11 | 0.12 | 0.10 | 0.14 | 0.10 | 0.13 | 0.09 |

**Table 16**: The predictions for $R(D^{(*)})$ using the fit results of the HQET parameters given in table 14. $a_1^{\mathcal{F}_2}$ is fixed using eq. 4.19. The additional error ($\Delta$) in the ratio $h_+/h_{A_1}$ (eq. 4.14) are considered as $1 \pm 0.1$ (for detail, see the text). Also, wherever applicable, the $\Delta_{31}$, $\Delta_{21}$ and $\Delta_{\mp}$, they all are taken as $1 \pm 0.2$. The details of the choices of $F_i(w)$ in different cases can be seen from the text.

| Parameters/ Observables | $F_i(w)$ in eq. 4.11 : $F_1(w)$ & $f(w)$ | | $F_i(w)$ in eq. 4.11 : $F_1(w)$ & $f(w)$ | | $F_i(w)$ in eq. 4.11 : $f_+(w)$ & $f_0(w)$ | | $F_i(w)$ in eq. 4.11 : $f_+(w)$ & $f_0(w)$ | |
|---|---|---|---|---|---|---|---|---|
| | case-3 | case-3 with $\Delta$s | case-4 | case-4 with $\Delta$s | case-5 | case-5 with $\Delta$s | case-6 | case-6 with $\Delta$s |
| $a_0^{\mathcal{F}_2}$ | 0.053(1) | 0.053(4) | 0.053(1) | 0.053(4) | 0.058(1) | 0.058(8) | 0.058(1) | 0.058(8) |
| $a_2^{\mathcal{F}_2}$ | 0.19(3) | 0.02(9) | 0.18(6) | 0.08(19) | -0.72(1) | -0.46(15) | -0.73(12) | -0.46(15) |
| $R(D)$ | 0.302(3) | 0.302(3) | 0.302(3) | 0.302(3) | 0.302(3) | 0.302(3) | 0.302(3) | 0.302(3) |
| $\boldsymbol{R(D^*)}$ | **0.255(5)** | **0.255(5)** | **0.257(5)** | **0.257(5)** | **0.258(5)** | **0.258(7)** | **0.260(5)** | **0.260(7)** |
| Corr($R(D)$ -$R(D^*)$) | 0.12 | 0.11 | 0.12 | 0.10 | 0.14 | 0.10 | 0.13 | 0.09 |

**Table 17**: The predictions for $R(D^{(*)})$ using the fit results of the HQET parameters given in table 15. The rest of the assumptions are same as that given in the caption of table 16.

17 are obtained by the use of the following synthetic data points (eq. 4.11 for $w = 1$) [4]:

$$F_2(1) = \begin{cases} \left(\frac{F_2(1)}{f(1)}\right)_{HQET} f(1) & \text{for cases 3 and 4,} \\ \left(\frac{F_2(w)}{f_+(1)}\right)_{HQET} f_+(1) & \text{for cases 5 and 6} \end{cases} \tag{4.16}$$

[4]We have checked that if we instead use $F_i(1) = F_1(1)$ (in cases 3 and 4), the value of $F_2(1)$ (and hence $a_0^{\mathcal{F}_2}$) remains exactly the same as that obatained with $F_i(1) = f(1)$. This is because both of $F_1(1)$ and $f(1)$ are independent of HQET parameters and, in our BGL fits, we used the relation $F_1(1) = (m_B - m_{D^*})f(1)$. While using $F_i(1) = f_0(1)$ (in cases 5 and 6), the values of $F_2(1)$ and $a_0^{\mathcal{F}_2}$ had changed only slightly (unchanged at the precision we are quoting our results) with respect to the scenario $F_i(1) = f_+(1)$.

In order to extract the other two coefficients, we have to use eq. 4.7 for values of $w$ other than 1, and the unitarity constraint

$$(a_0^{\mathcal{F}_2})^2 + (a_1^{\mathcal{F}_2})^2 + (a_2^{\mathcal{F}_2})^2 < 1. \tag{4.17}$$

Naturally, the extracted values of $a_1^{\mathcal{F}_2}$ and $a_2^{\mathcal{F}_2}$ will be sensitive to the other HQET parameters along with $\eta(1)$. However, in order to reduce the impact of the HQET parameters on the final results, we use the QCD relation between the form factors:

$$F_2(q^2 = 0) = \frac{2F_1(q^2 = 0)}{m_B^2 - m_{D^*}^2}. \tag{4.18}$$

The coefficients of $F_1(z)$ are obtained from the BGL fits, and hence one of the coefficients in $F_2(z)$ can be written in terms of the coefficients of $F_1(z)$ and the rest of the coefficients in $F_2(z)$ using the above relation, e.g.,

$$a_1^{\mathcal{F}_2} = 71.3906a_0^f + 23.9092a_1^{\mathcal{F}_1} + 1.34087a_2^{\mathcal{F}_1} - 17.8312a_0^{\mathcal{F}_2} - 0.0560815a_2^{\mathcal{F}_2}. \tag{4.19}$$

Note that, $a_1^{\mathcal{F}_2}$ is highly sensitive to the extracted value of $a_0^{\mathcal{F}_2}$. However, for small values of $a_2^{\mathcal{F}_2}$ ( $\ll 1$), $a_1^{\mathcal{F}_2}$ has very little dependency on it. Also, $R(D^*)$ is relatively less sensitive to the coefficient $a_2^{\mathcal{F}_2}$ and its predictions do not change depending on the changes in $a_2^{\mathcal{F}_2}$. Still, for completeness, we have extracted this coefficient from eq. 4.7 by a fit using the synthetic data points for $F_2(w)$ for $w = 1.03$, 1.06, 1.09 and 1.12. As explained earlier, these $F_2(w)$ values are obtained using the following relations [5]:

$$F_2(w) = \left\{ \begin{array}{l} \left(\frac{F_2(w)}{f(w)}\right)_{HQET} f(w), \\ \left(\frac{F_2(w)}{F_1(w)}\right)_{HQET} F_1(w) \end{array} \right\} \text{for both the cases 3 \& 4} \tag{4.20}$$

and

$$F_2(w) = \left\{ \begin{array}{l} \left(\frac{F_2(w)}{f_+(w)}\right)_{HQET} f_+(w), \\ \left(\frac{F_2(w)}{f_0(w)}\right)_{HQET} f_0(w) \end{array} \right\} \text{for both the cases 5 \& 6.} \tag{4.21}$$

The fitted values of $a_2^{\mathcal{F}_2}$ are shown in table 16 and 17. The coefficients obtained in this way, and hence $R(D^*)$, will be mostly sensitive to $\eta(1)$. Therefore, the final results will be less dependent on the HQET parameters.

We present our final results for $R(D^{(*)})$ in table 16. The prediction for $R(D)$ is consistent with the one obtained in an earlier analysis [11]. Our important results are marked in bold. Amongst these, the one obtained in case-4 (with $\Delta$) can be considered as our best result. The reasons are following:

[5] We had also done the analysis using one normalization at a time. As for example, in both the cases 3 and 4, we had choosen $F_i(w)$ to be either of $f(w)$ or $F_1(w)$. Similarly, for the cases 5 and 6, we had replaced $F_i(w)$ either by $f_+(w)$ or $f_0(w)$. In the specific cases, we did not get any considerable changes in the predictions of $R(D^*)$ due to the different choices of the normalization of $F_2(w)$, also the predictions were in complete agreement with those given in table 16 and 17 which are obtained from the mixed normalizations. However, for completeness, we have presented our results using mixed normalizations, it adds more inputs to the fits.

- In this case, the HQET parameters are fitted with all available inputs.

- $R(D^*)$ has been extracted using the HQET relations $F_2(w)/f(w)$ and $F_2(w)/F_1(w)$, which are less sensitive to the HQET parameters (even $\eta(1)$) as compared to the other ratios, like $F_2(w)/f_{+/0}(w)$.

We note that across all the cases, the overall uncertainties in predictions of $R(D^*)$ with the known corrections in HQET, are roughly 2%. However, when we incorporate the additional unknown corrections ($\Delta$s) conservatively in the HQET form factor ratios (from the fit), the uncertainties in cases 5 and 6 are increased to 3%, while those in cases 3 and 4 remain the same. We have checked that in the cases 5 and 6 (with $\Delta$s), the overall uncertainties in the predictions of $R(D^*)$ are 4% without using the QCD relation between the form factors, while those for the cases 3 and 4 (with $\Delta$s) are roughly 3%. Due to the QCD relation, the errors have reduced by 1% in all these four cases with conservative $\Delta$s, which is due to a negative correlation between $a_0^{\mathcal{F}_2}$ and $a_1^{\mathcal{F}_2}$; for details see eq. 4.19. The increase in errors for the cases 5 and 6 (with $\Delta$s) with respect to the cases 3 and 4 (with $\Delta$s) can be understood in the following way. The form factor ratios used in cases 5 and 6 have additional sources of errors compared to those used in the cases 3 and 4. As can be seen from eqs. 4.12, 4.13 and 4.14, in our analysis, the ratios $F_2(w)/f(w)$ and $F_2(w)/F_1(w)$ are sensitive only to $\Delta_{21}$ and $\Delta_{31}$ while the ratios $F_2(w)/f_{+/0}(w)$ are sensitive to $\Delta_{21}$, $\Delta_{31}$, $\Delta_{\mp}$, and the additional unknown corrections associated with the ratio $h_-/h_{A_1}$. Our predictions for $R(D^*)$ are consistent with the one obtained in [19].

## 5 Summary

In this article, we analyze the decay modes $B \to D\ell\nu_\ell$ and $B \to D^*\ell\nu_\ell$ with the complete sets of available data on the angular (wherever applicable) as well $w$-bins. The CKM element $V_{cb}$ have been extracted from the analysis of the above mentioned decay modes independently, as well as from a combined analysis. We have done the analysis using the CLN and BGL parameterizations of the form factors. Our best results are $|V_{cb}| = 39.77 \pm 0.89$ in the CLN parameterization of the form factors and that in the case of BGL is $|V_{cb}| = 40.90 \pm 0.94$. These are so far the most precise results obtained in the analysis of the exclusive decays. In the combined analysis of the data, our prediction for $R(D)$ in the CLN parameterization of the form factors is given by $R(D) = 0.304 \pm 0.003$, while using BGL parameterization, we obtain $R(D) = 0.302 \pm 0.003$ for $N = 2$ and $R(D) = 0.299 \pm 0.004$ for $N = 3$, without using the strong unitarity constraints. These are all consistent with earlier predictions.

Also, we predict $R(D^*)$ with the available known corrections at order $\mathcal{O}(\Lambda_{QCD}/m_{b,c}, \alpha_s)$ in the HQET relations between the form factors, and we obtain $R(D^*) = 0.259 \pm 0.003$ in the CLN parameterization, while that in the BGL parameterization of the form factors is given by $R(D^*) = 0.257 \pm 0.005$. For completeness, we parameterized the unknown corrections in the ratios of the HQET form factors by introducing additional factors ($\Delta$s), and fit them from the available data and lattice. After incorporating all the fit results, in

the CLN method, we obtain $R(D^*) = 0.259 \pm 0.006$, while in the BGL method, our best result is $R(D^*) = 0.257 \pm 0.005$.

## 6 Acknowledgement

We would like to thank Paolo Gambino for providing us the complete data file from Belle and having some useful discussions.

## References

[1] J. Chay, H. Georgi and B. Grinstein, Phys. Lett. B **247**, 399 (1990); I. I. Y. Bigi, M. A. Shifman, N. Uraltsev and A. I. Vainshtein, Phys. Rev. D **59**, 054011 (1999) [hep-ph/9805241]; I. I. Y. Bigi, M. A. Shifman, N. G. Uraltsev and A. I. Vainshtein, Int. J. Mod. Phys. A **9**, 2467 (1994) [hep-ph/9312359].

[2] N. Isgur and M. B. Wise, Phys. Lett. B **232**, 113 (1989). M. A. Shifman and M. B. Voloshin, Sov. J. Nucl. Phys. **47**, 511 (1988) [Yad. Fiz. **47**, 801 (1988)].

[3] A. Alberti, P. Gambino, K. J. Healey and S. Nandi, Phys. Rev. Lett. **114**, no. 6, 061802 (2015) [arXiv:1411.6560 [hep-ph]]; P. Gambino, K. J. Healey and S. Turczyk, Phys. Lett. B **763**, 60 (2016) [arXiv:1606.06174 [hep-ph]].

[4] Y. Amhis *et al.*, arXiv:1612.07233 [hep-ex].

[5] I. Caprini, L. Lellouch and M. Neubert, Nucl. Phys. B **530**, 153 (1998) doi:10.1016/S0550-3213(98)00350-2 [hep-ph/9712417].

[6] C. G. Boyd, B. Grinstein and R. F. Lebed, Phys. Rev. D **56**, 6895 (1997) doi:10.1103/PhysRevD.56.6895 [hep-ph/9705252].

[7] D. Bigi, P. Gambino and S. Schacht, Phys. Lett. B **769**, 441 (2017) doi:10.1016/j.physletb.2017.04.022 [arXiv:1703.06124 [hep-ph]]; B. Grinstein and A. Kobach, Phys. Lett. B **771**, 359 (2017) [arXiv:1703.08170 [hep-ph]].

[8] A. Abdesselam *et al.* [Belle Collaboration], "Precise determination of the CKM matrix element $|V_{cb}|$ with $\bar{B}^0 \to D^{*+} \ell^- \bar{\nu}_\ell$ decays with hadronic tagging at Belle," arXiv:1702.01521 [hep-ex].

[9] S. Aoki *et al.*, Eur. Phys. J. C **77**, no. 2, 112 (2017) doi:10.1140/epjc/s10052-016-4509-7 [arXiv:1607.00299 [hep-lat]].

[10] S. Fajfer, J. F. Kamenik and I. Nisandzic, Phys. Rev. D **85**, 094025 (2012) doi:10.1103/PhysRevD.85.094025 [arXiv:1203.2654 [hep-ph]].

[11] D. Bigi and P. Gambino, Phys. Rev. D **94**, no. 9, 094008 (2016) doi:10.1103/PhysRevD.94.094008 [arXiv:1606.08030 [hep-ph]].

[12] J. A. Bailey *et al.* [MILC Collaboration], "$B \to D\ell\nu$ form factors at nonzero recoil and $|\mathrm{V}_{cb}|$ from 2+1-flavor lattice QCD," Phys. Rev. D **92**, no. 3, 034506 (2015) doi:10.1103/PhysRevD.92.034506 [arXiv:1503.07237 [hep-lat]].

[13] H. Na *et al.* [HPQCD Collaboration], "$B \to Dl\nu$ form factors at nonzero recoil and extraction of $|V_{cb}|$," Phys. Rev. D **92**, no. 5, 054510 (2015) Erratum: [Phys. Rev. D **93**, no. 11, 119906 (2016)] doi:10.1103/PhysRevD.93.119906, 10.1103/PhysRevD.92.054510 [arXiv:1505.03925 [hep-lat]].

[14] F. U. Bernlochner, Z. Ligeti, M. Papucci and D. J. Robinson, Phys. Rev. D **95**, no. 11, 115008 (2017) doi:10.1103/PhysRevD.95.115008 [arXiv:1703.05330 [hep-ph]].

[15] M. Neubert, Z. Ligeti and Y. Nir, Phys. Lett. B **301**, 101 (1993) doi:10.1016/0370-2693(93)90728-Z [hep-ph/9209271].

[16] M. Neubert, Z. Ligeti and Y. Nir, Phys. Rev. D **47**, 5060 (1993) doi:10.1103/PhysRevD.47.5060 [hep-ph/9212266].

[17] "Instant workshop on $B$ meson anomalies" presentation by Stefan Schacht, https://indico.cern.ch/event/633880/timetable/

[18] R. Glattauer *et al.* [Belle Collaboration], "Measurement of the decay $B \to D\ell\nu_\ell$ in fully reconstructed events and determination of the Cabibbo-Kobayashi-Maskawa matrix element $|V_{cb}|$," Phys. Rev. D **93**, no. 3, 032006 (2016) doi:10.1103/PhysRevD.93.032006 [arXiv:1510.03657 [hep-ex]].

[19] D. Bigi, P. Gambino and S. Schacht, arXiv:1707.09509 [hep-ph].

[20] See the supplemental material at the APS site, or in the ancilliary files of arXiv preprint of ref. [18].

[21] N. Uraltsev, Phys. Lett. B **585**, 253 (2004) doi:10.1016/j.physletb.2004.01.053 [hep-ph/0312001].

[22] J. A. Bailey *et al.* [Fermilab Lattice and MILC Collaborations], "Update of $|V_{cb}|$ from the $\bar{B} \to D^*\ell\bar{\nu}$ form factor at zero recoil with three-flavor lattice QCD," Phys. Rev. D **89**, no. 11, 114504 (2014) doi:10.1103/PhysRevD.89.114504 [arXiv:1403.0635 [hep-lat]].

[23] S. Faller, A. Khodjamirian, C. Klein and T. Mannel, Eur. Phys. J. C **60**, 603 (2009) doi:10.1140/epjc/s10052-009-0968-4 [arXiv:0809.0222 [hep-ph]].